

# KPG: Key Propagation Graph Generator for Rumor Detection based on Reinforcement Learning

Yusong Zhang\*  
The Chinese University of Hong Kong  
Hong Kong  
yusongzhang@cuhk.edu.hk

Kun Xie\*  
The Chinese University of Hong Kong  
Hong Kong  
xiekun@se.cuhk.edu.hk

Xingyi Zhang  
The Chinese University of Hong Kong  
Hong Kong  
xyzhang@se.cuhk.edu.hk

Xiangyu Dong  
The Chinese University of Hong Kong  
Hong Kong  
xydong@se.cuhk.edu.hk

Sibo Wang<sup>†</sup>  
The Chinese University of Hong Kong  
Hong Kong  
swang@se.cuhk.edu.hk

## ABSTRACT

The proliferation of rumors on social media platforms during significant events, such as the US elections and the COVID-19 pandemic, has a profound impact on social stability and public health. Existing approaches for rumor detection primarily rely on propagation graphs to enhance model effectiveness. However, the presence of noisy and irrelevant structures during the propagation process limits the efficacy of these approaches. To tackle this issue, techniques such as weight adjustment and data augmentation have been proposed. However, these techniques heavily depend on rich original propagation structures, thus hindering performance when dealing with rumors that lack sufficient propagation information in the early propagation stages. In this paper, we propose *Key Propagation Graph Generator (KPG)*, a novel reinforcement learning-based rumor detection framework that generates contextually coherent and informative propagation patterns for events with insufficient topology information, while also identifies indicative substructures for events with redundant and noisy propagation structures. KPG consists of two key components: the *Candidate Response Generator (CRG)* and the *Ending Node Selector (ENS)*. CRG learns the latent distribution from refined propagation patterns, filtering out noise and generating new candidates for ENS. Simultaneously, ENS identifies the most influential substructures within propagation graphs and generates training data for CRG. Moreover, we introduce an end-to-end framework that utilizes rewards to guide the entire training process via a pre-trained graph neural network. Extensive experiments conducted on four datasets demonstrate the superiority of our KPG compared to the state-of-the-art approaches.

\*Both authors contributed equally to the paper.

<sup>†</sup>Sibo Wang is the corresponding author.

Permission to make digital or hard copies of all or part of this work for personal or classroom use is granted without fee provided that copies are not made or distributed for profit or commercial advantage and that copies bear this notice and the full citation on the first page. Copyrights for components of this work owned by others than ACM must be honored. Abstracting with credit is permitted. To copy otherwise, or republish, to post on servers or to redistribute to lists, requires prior specific permission and/or a fee. Request permissions from [permissions@acm.org](mailto:permissions@acm.org).

Conference acronym 'XX, June 03–05, 2018, Woodstock, NY

© 2018 Association for Computing Machinery.  
ACM ISBN 978-1-4503-XXXX-X/18/06...\$15.00  
<https://doi.org/XXXXXXXX.XXXXXXX>

## ACM Reference Format:

Yusong Zhang, Kun Xie, Xingyi Zhang, Xiangyu Dong, and Sibow Wang. 2018. KPG: Key Propagation Graph Generator for Rumor Detection based on Reinforcement Learning. In *Proceedings of Make sure to enter the correct conference title from your rights confirmation email (Conference acronym 'XX)*. ACM, New York, NY, USA, 11 pages. <https://doi.org/XXXXXXXX.XXXXXXX>

## 1 INTRODUCTION

As one of the primary mediums for information dissemination, social media eliminates the temporal and spatial constraints on individual communication and facilitates the spread of information. However, the popularity of certain topic on social media often leads to the propagation of intentional or unintentional misinformation [60], bringing negative impact to individual health and social stability [49, 58]. Unfortunately, individuals exposed to unverified information have difficulty in distinguishing between truth and falsehood, and may unknowingly contribute to its further dissemination through social media [33, 60]. Therefore, there is a growing demand for automatic rumor detection.

In recent years, rumor detection approaches have gradually shifted from traditional machine learning approaches [29, 32, 46, 59] that require manual definition of content, structural, or information source features, to deep learning approaches [6, 12, 17, 22, 27, 30, 38, 42, 44, 45, 55, 56]. Notably, *graph neural network (GNN)*-based rumor detectors have achieved superb performance. These models leverage both the textual contents and the topology of propagation graphs that represents the spread of claims on social networks. In these graphs, nodes represent comments or retweets of the root claim, while edges capture the relationships of commenting and retweeting among these posts. Although the use of propagation information improves the accuracy of rumor detection to some extent, the presence of irrelevant or untrustworthy comments on social networks significantly impairs the reliability of the propagation graphs when identifying claims [38, 44].

To address this challenge, techniques such as weight adjustment [43, 44] and data augmentation [12, 24, 38] have been introduced. However, these strategies rely on graphs with abundant structural information, which is often not met by rumors (particularly in the early stages of spreading) in real-world social networks. To clarify, early-stage rumor detection is vital for controlling the negative effects of misinformation. Yet, as pointed out in [25, 57], existing approaches struggle to address events with inadequate topological

information effectively. The absence of distinguishable structures on small graphs is the primary reason leading to the unsatisfactory results [25]. Therefore, how to design an effective rumor detector that can deal with not only noisy propagation graphs with irrelevant comments, but also small propagation graphs at the early stage of spreading, remains an unresolved problem.

Motivated by this, in this paper, we propose KPG<sup>1</sup> to generate enhanced key propagation graphs for rumor veracity classification. Our KPG comprises two key components: the *Candidate Response Generator (CRG)* and the *Ending Node Selector (ENS)*, as shown in Figure 1. Firstly, to deal with the events where propagation graphs are too small to provide sufficient candidates for selection, we propose CRG module based on the *conditional variational auto-encoder (CVAE)* [35]. CRG generates new responses that are coherent with the structure and contextual information present in the graph. These responses are generalized from realistic yet refined from noise propagation patterns, with the aim of enhancing the discrimination potential of the augmented graphs. Next, ENS explores the candidate graph from both local and global perspectives and identifies the key propagation graph by selecting critical nodes iteratively from the candidate set. Rather than choosing nodes based on semantic relevance of comments, ENS prioritizes nodes that indicate the veracity of the claim. Using GCN [6, 20] as the backbone, ENS evaluates each node based on the contribution of its feature and topology information to the classification performance of the event. By incorporating these two modules, our KPG can not only select distinguishable key patterns from the original noisy propagation graphs, but also expand small propagation graphs with informative new comments, thereby improving the overall model performance on the rumor detection task.

We further incorporate a *reinforcement learning (RL)* framework to integrate the candidate node generation and key node selection process with graph classification accuracy. To achieve this, we design rewards based on the classification accuracy obtained from a pre-trained GCN classifier [6]. Specifically, we offer rewards for generated new responsive features that demonstrate superior performance compared to the original features in terms of classification accuracy. Besides, we encourage the selection of nodes that enhance the discriminative capability of the graph and maximize the expected accumulative performance improvement in the future.

Finally, we develop the KPG as an end-to-end framework. It trains the ENS and the CRG alternately, allowing both components to generate intermediate results for each other and be optimized iteratively. On the one hand, the CRG generates new responses to supplement the candidate set of the ENS, enabling ENS to overcome limitations imposed by insufficient input information. On the other hand, the key patterns identified by ENS serve as training samples for CRG, facilitating the extraction of latent variable distributions from realistic and distinguishable propagation patterns. The final key propagation graphs are then utilized to train a downstream GCN classifier for the rumor detection task.

In summary, our contributions are listed as follows:

- We propose a novel KPG model, including two interdependent modules, which can augment small graphs with contextually

**Table 1: Frequently used notations.**

Notations	Descriptions
$r, s, y_s$	Source post, event, and its ground-truth label.
$G, V, E, X$	Input propagation graph, node set, edge set, and feature matrix.
$g_t, G_t$	Key propagation graph and candidate graph at step $t$ .
$v_t, e_t$	The newly added node and edge at step $t$ .
$C_{t+1}$	Candidate set for ENS to select $v_t$ .
$\epsilon, \gamma$	Trade-off parameter and threshold of candidate sets.
$l$	The max step in modified Rollout.
$\tau$	Controlling the max generation step.

relevant, reliable responses and precisely select the indicative key nodes considering both features and structural information.

- We incorporate the RL framework into the propagation graph-based rumor detection. The carefully designed rewards improve the graph discriminability during key graph generation process.
- Extensive experiments<sup>2</sup> show that KPG achieves state-of-the-art performance on the rumor detection task.

## 2 PRELIMINARIES

### 2.1 Notation

Let  $s = \{r, G = (V, E, X)\}$  denote an event, where  $r$  is the source post of the event, and  $G$  indicates the propagation graph of the source post on the social media.  $G$  is directed and also an acyclic tree rooted at the source post  $r$ . The node set  $V = \{r, v_1, v_2, \dots, v_{n_s-1}\}$  contains all  $n_s$  comments and retweets in the propagation process. The edge set  $E = \{(v_i, v_j) | v_i, v_j \in V\}$  represents the propagating relation between posts, i.e., if  $v_j$  is a comment or retweet of  $v_i$ , then there exists a directed edge  $(v_i, v_j)$  from  $v_i$  to  $v_j$ .  $X \in \mathbb{R}^{n_s \times d}$  contains the initial features of posts in the event. Each row of the feature matrix  $X[v_i]$  is a  $d$ -dimension feature vector of the corresponding post  $v_i$ . Frequently used notations in this paper are listed in Table 1.

Let  $y_s \in \mathcal{Y}$  be the label of the event  $s$ , which indicates the veracity of the event. The label set  $\mathcal{Y}$  consists of non-rumors, false rumors, true rumors, and unverified rumors. Some datasets contain only two classes, i.e., rumors and non-rumors. Given a set of events  $\{s_0, s_1, \dots\}$  obtained from social networks, the goal of rumor detection is to predict the veracity of each event.

### 2.2 Related Work

**Graph-based Rumor Detection.** A line of research studies [13, 52, 53] construct heterogeneous graphs of publishers, tweets, and users to combine both local and global relationships. Based on such heterogeneous graphs, a series of models have been proposed. For instance, GCAN [26] uses a dual co-attention mechanism to provide reasonable explanations by learning features from four aspects. Cui et al. [8] propose encoding metapaths from heterogeneous graphs. FinerFact [14] reasons for important evidence from a constructed claim-evidence graph using the mutual reinforcement mechanism [10]. SureFact [48] further leverages RL to measure the importance

<sup>1</sup>Key Propagation Graph Generator

<sup>2</sup>Code available at <https://anonymous.4open.science/r/KPG-A279/README.md>

of nodes and conducts subgraph reasoning. Note that some additional information, such as news-user discussion graphs, user-user interaction graphs, news-posts similarity graphs, etc, used to construct the heterogeneous graphs is not included in the datasets we used. To ensure a fair comparison, we exclude these methods in our experiments.

Another line of research studies adopts GCN to enhance the particular exploitation of the propagation graphs of rumors. For example, BiGCN [6] employs GCN on both top-down and bottom-up propagation graphs. EBGCN [44] and FGCN [43] suggest adjusting the weight of each edge to reflect the intensity of interactions between comments. Models like RDEA [12], GACL [38], and TrustRD [24] and others [27, 54] employ data augmentation strategies like edge perturbation and masking to improve the robustness of the model through contrastive learning. AARD [36] generates position-aware adversarial responses to improve the vulnerability of models.

However, current models heavily rely on the original topology information to fight the untrustworthy comments in the propagation graphs. Thus, these strategies are invalid in the case of small graphs with insufficient structural information. In contrast, our KPG proposes two interdependent modules, generating key propagation patterns for propagation graphs of varied sizes and achieving superb performance, as to be shown in our experiments.

**Graph Generation.** The goal of this task is to generate new realistic graphs by learning the distribution of the observed graphs. Graph generative models can be classified based on their generation process, which can be either one-shot or sequential [11]. GraphRNN [51], MolecularRNN [31], and DeepGMG [23] generate realistic molecular graphs based on auto-regressive models, while GCPN [50] and related methods [15, 16, 34, 41] formulate the problem as a Markov decision process, generating molecular graphs step-by-step. In addition, there exist methods focusing on mining critical subgraphs that are crucial for downstream tasks. For instance, SMG [47] identifies task-relevant structures from a sequence of subgraphs through a differentiable soft mask mechanism. CAL [37] employs attention modules to extract critical features by distinguishing between causal and shortcut features. AdaSNN [21] detects critical structures by using a reinforced module that maximizes global-aware and label-aware mutual information.

However, existing graph generators mainly overlook the connections between text characteristics and spreading patterns. In contrast, our approach takes into account this crucial aspect by dynamically updating candidate sets and effectively integrating node features with structural information when generating key propagation graphs. KPG can be viewed as a combination of new graph generation and critical subgraph mining. On the one hand, it generates realistic responses following the learned latent distribution of filtered text pairs. This capability enables KPG to effectively handle the limited size of graphs in the early propagation stage. On the other hand, KPG identifies the critical substructures from the enhanced graphs, mitigating the impact of unreliable comments.

### 3 KEY PROPAGATION GRAPH GENERATOR

In this section, we present our KPG model, which consists of two key components: *Candidate Response Generator (CRG)* and *End Node Selector (ENS)*. To address the limitations of existing models in

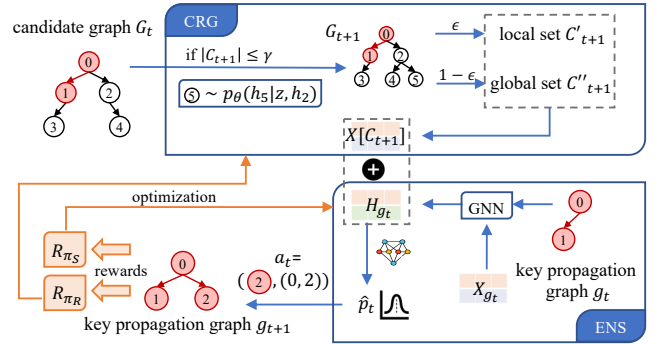


Figure 1: Key propagation graph generation process.

handling small input graphs with insufficient topological information, we propose the CRG module to generate realistic and reliable responses to expand the graph. Subsequently, ENS generates a probability distribution for each node, indicating the likelihood of the node being selected during the step-by-step construction of the key propagation graph. Specifically, we select the propagation patterns that are critical and indicative for classification, while filtering out those irrelevant and noisy comments. We utilize an RL framework to design rewards for both two modules, further enhancing the model performance on the generated key propagation graphs. With the guidance of carefully designed rewards, the classification accuracy of the key propagation graph in the current state is encouraged to surpass that of its preceding state, ensuring continuous enhancement throughout the generation process.

The rest of this section is arranged as follows. We first formulate the key propagation generation problem with the reinforcement learning framework in Section 3.1. Then, we elaborate the two key components, CRG and ENS, in Section 3.2 and 3.3, respectively. Finally, we illustrate the reward functions used for guiding CRG and ENS, and present the complete learning algorithm in 3.4.

#### 3.1 Problem Formulation

As previously mentioned, we employ the RL framework to solve the key propagation generation problem. In a typical RL framework, there are four essential components: state, action, policy, and reward. Next, we provide a detailed explanation of the definition of these components in our problem. Broadly speaking, our CRG and ENS serve as the policy in the RL framework. Specifically, ENS generates a probability distribution of available actions, which determines the transition from the current state to the next state. The CRG is closely integrated with ENS by providing informative and discriminating candidates for ENS. Finally, both CRG and ENS are optimized by rewards to maximize the expected cumulative performance improvement.

**State.** The state at step  $t$  is the key propagation graph, denoted as  $g_t = \{V_{g_t}, E_{g_t}, X_{g_t}\}$ , where  $V_{g_t}$  and  $E_{g_t}$  denotes the node set with  $n_t$  nodes and the edge set with  $m_t$  edges, respectively.  $X_{g_t} \in \mathbb{R}^{n_t \times d}$  is the feature matrix. The initial state  $g_0$  contains only the root node  $r$  and its feature  $X[r]$ :

$$g_0 = (V_{g_0} = \{r\}, E_{g_0} = \{\}, X_{g_0} = X[r]).$$

At the right bottom of Figure 1, we present a toy example of key propagation graph  $g_t$  with two nodes at step  $t$ .

**Action.** At step  $t$ , action  $a_t = (v_t, e_t)$ , where  $v_t$  and  $e_t$  represents the node and edge to be added to  $g_t$  for generating a new key propagation graph  $g_{t+1}$ , respectively. Specifically, if there are insufficient nodes as candidates, CRG is invoked to expand the candidate graphs; otherwise, the candidate graphs keep unchanged. We denote the candidate graph at step  $t$  as  $G_t = \{V_{G_t}, E_{G_t}, X_{G_t}\}$ , which is initialized as the input propagation graph when  $t = 0$ . Then, based on the candidate graph, ENS is employed to produce probability scores indicating the importance of each candidate node in terms of classifying the source event. According to the probability score, the node  $v_t$  and corresponding connecting edge  $e_t$  are selected in action  $a_t$ . Figure 1 illustrates the selection process of action  $a_t = (2, (0, 2))$ .

**Policy.** The policy consists of two parts: End Node Selector  $\pi_S(\cdot)$  and Candidate Response Generator  $\pi_R(\cdot)$ . ENS  $\pi_S(\cdot)$  takes the current key propagation graph  $g_t$  as input, and outputs the probability distribution of candidates being selected in this step. If the number of candidates is smaller than a pre-defined threshold, CRG is invoked before ENS to expand the candidate graph. To be specific, CRG  $\pi_R(\cdot)$  generates effective and diverse responses for the sampled node in the current candidate graph  $G_t$ . The generation process and the corporation between  $\pi_R$  and  $\pi_S$  are shown in Figure 1.

**Reward.** The rewards assigned to  $\pi_S(\cdot)$  and  $\pi_R(\cdot)$  are designed to increase the discriminate capacity of generated key graphs. Specifically, for CRG  $\pi_R(\cdot)$ , the model is encouraged to generate more informative and discriminate features than the former input features in terms of classification accuracy. For ENS  $\pi_S(\cdot)$ , we aim to maximize the improvement of classification performance brought by incorporating  $(v_t, e_t)$ . Besides, we consider not only the performance improvement in this step, but also the potential improvement in the future steps. If  $\pi_R(\cdot)$  and  $\pi_S(\cdot)$  are well-trained, these modules will remain in the current states. The encouragement is accomplished by multiplying the loss functions with the corresponding rewards, which is smaller than one if the action works as expected. Otherwise, we will penalize the two modules and push them away from the current state. At the left bottom of Figure 1, the rewards for  $\pi_R$  and  $\pi_S$  are derived based on the updated stage  $g_{t+1}$ , and are used to optimize these modules.

**Overall Workflow.** We present the overall workflow of our KPG at step  $t$  in Figure 1. Specifically, at step  $t$ , if the number of candidates is less than  $\gamma$ , CRG is invoked to generate new responses drawn from a learned latent distribution. Then, we select candidates by balancing local and global perspectives based on a probability  $\epsilon$ . Next, ENS encodes the current graph  $g_t$  with a GNN model and concatenates the graph representation and candidate features together. A fully connected layer is utilized to derive the probability of each available action  $a_t$ . Graph  $g_{t+1}$  is updated based on  $a_t$ . Finally, the rewards are computed to optimize CRG and ENS.

### 3.2 Candidate Response Generator

In this section, we present the Candidate Response Generator component  $\pi_R(\cdot)$ . Existing data augmentation approaches primarily focus on perturbing the input structure. However, perturbation-based models struggle with small propagation graphs that inherently

lack sufficient topology and feature information. In contrast, CRG presents a novel approach by introducing entirely new content as responses to the given nodes, augmenting the graph in a contextually coherent manner. Specifically, CRG is designed to support event classification from three aspects:

- (i) Contextually coherent: generating responses directly relevant to the original context of the graph;
- (ii) Realistic yet refined from noise: generating responses that reflect real-world social network propagation patterns while robust to noisy and irrelevant comments;
- (iii) Discriminate: generating distinct responses contributing to rumor detection and downstream performance improvement.

Among these objectives, we achieve (iii) through carefully designed rewards, which are discussed in detail in Section 3.4. The mechanisms behind (i) and (ii) are elaborated in this section.

To accomplish objective (i), we construct our CRG based on *conditional variational auto-encoders (CVAE)* [35]. This extension of the traditional VAE [19] incorporates condition variables to generate new responses conditioned on the given context following a latent distribution. By extracting this distribution from real-world propagation patterns, CVAE can effectively generate responses that maintain contextual coherence.

To accomplish objective (ii), we utilize all currently identified key propagation graphs rather than the original input graphs as training data for CRG, filtering out noisy and irrelevant comments. This approach allows CRG to learn from propagation patterns that significantly contribute to the classification task and alleviate the impact of noisy comments.

**CRG Component.** Let  $(u, v) \in E_{g_t}$ , where  $g_t$  is a key propagation graph that has been identified at step  $t$ . The node pair  $(u, v)$  can be seen as a context-response pair, where  $u$  denotes the context and  $v$  denotes the response. We initially employ a GRU [7] to encode the text sequences of  $u$  and  $v$  into embeddings  $\mathbf{h}_u$  and  $\mathbf{h}_v$ , respectively. Since the same context may appear across various events while their responses can differ significantly, we augment the representation of  $u$  with its source post  $r$  to alleviate such a one-to-many problem. The embedding of the source post  $r$  is obtained by another GRU:

$$\mathbf{h}_u = \text{GRU}_1(\text{text}(u)) \parallel \text{GRU}_2(\text{text}(r)), \mathbf{h}_v = \text{GRU}_1(\text{text}(v)),$$

where  $\text{text}(\cdot)$  represents obtaining the text sequence of the node. Next,  $\mathbf{h}_u$  and  $\mathbf{h}_v$  are fed into the CVAE model. Specifically, CVAE includes an encoder  $q_\phi(\mathbf{z}|\mathbf{h}_u, \mathbf{h}_v)$  and a decoder  $p_\theta(\mathbf{h}_v|\mathbf{z}, \mathbf{h}_u)$  with latent space representation  $\mathbf{z}$ , which is assumed to follow a normal distribution with mean  $\boldsymbol{\mu}$  and variance  $\sigma^2$ , i.e.,  $\mathbf{z} \sim \mathcal{N}(\boldsymbol{\mu}, \sigma^2)$ . In the encoding phase, the embeddings  $\mathbf{h}_u$  and  $\mathbf{h}_v$  is concatenated and fed into the MLP model to extract representation  $\mathbf{z}$ :

$$\boldsymbol{\mu} = \text{MLP}_1(\mathbf{h}_u \parallel \mathbf{h}_v), \sigma^2 = \text{MLP}_2(\mathbf{h}_u \parallel \mathbf{h}_v).$$

A sample  $\mathbf{z}' \sim q_\phi(\mathbf{z}|\mathbf{h}_u, \mathbf{h}_v)$  is drawn from the latent space distribution by reparameterization trick [35]. Then, the decoder reconstructs the response  $\mathbf{h}_v$  based on the context  $\mathbf{h}_u$  and  $\mathbf{z}'$ :

$$\hat{\mathbf{h}}_v = \text{MLP}_3(\mathbf{z}' \parallel \mathbf{h}_u).$$

During the training phase of CRG, the difference between input response  $\mathbf{h}_v$  and the reconstructed response  $\hat{\mathbf{h}}_v$  is employed as the optimization loss, along with another KL-divergence loss. More

details about the training of CRG are presented in Section 3.4. During the inference phase of CRG, the CVAE model is invoked to generate a response for a given context node. The output response embedding is then utilized as the initial state of a GRU model to produce the corresponding text sequence word by word.

Recap from Section 3.1 that, at each step  $t$  during the key graph generation process, the CRG is first invoked to augment the candidate graph. We set a threshold  $\gamma$  for the size of the candidate set. If the number of candidate nodes is more than  $\gamma$ , the candidate graph remains unchanged. If the number of candidate nodes is less than  $\gamma$ , CRG is invoked to generate responses for the sampled candidate nodes. The generated new response nodes are utilized to expand the candidate set. After that, ENS is employed to identify the next key node for propagation based on the updated candidate set.

### 3.3 Ending Node Selector

In this section, we present the Ending Node Selector  $\pi_S(\cdot)$ . At each step  $t$ , we first adopt CRG to update the candidate graph from  $G_t$  to  $G_{t+1}$ . Subsequently, based on the current key propagation graph  $g_t$  and the candidate graph  $G_{t+1}$ , ENS predicts the probabilities of candidates being selected by action  $a_t$ . These probabilities are derived based on the potential improvement of the event classification performance, i.e., ENS tends to choose the node that can contribute the most to improving the classification accuracy and disregard those irrelevant to the veracity of the event.

To achieve this, ENS first encodes the current key propagation graph  $g_t$  using a GCN model [20]. Then, we aggregate the features of candidates and the embedding of current  $g_t$  through a concatenate operation. This approach enables us to consider both the feature and topology information of candidates during the subsequent assessment. Finally, the resulting probability distribution highlights the nodes that have the potential to further enhance the model performance on  $g_t$ .

**ENS Component.** Specifically, to incorporate both textual and topological information into the final representation of  $g_t$ , we aggregate neighbor features through the graph structure via a GCN:

$$H_{g_t} = \text{GCN}(\hat{A}_{g_t}, X_{g_t}),$$

where  $\hat{A}_{g_t}$  is the normalized adjacency matrix of  $g_t$  with self-loop. Next, we concatenate  $H_{g_t}$  with the feature of candidates and employ a fully connected layer to derive the probability distribution, indicating the likelihood of each candidate being selected.

We consider the following two types of candidates when selecting candidate nodes. The first type consists of the nodes that belong to the candidate graph  $G_{t+1}$  and are connected to nodes in the current key propagation graph  $g_t$ . Since the propagation graph is tree-structured, these nodes, referred to as *local candidates*, are also the children of  $g_t$ :

$$C'_{t+1} = \{v \in V_{G_{t+1}} | (u, v) \in E_{G_{t+1}}, u \in V_{g_t}\}.$$

The second type of nodes comprises those that exist in the candidate graph  $G_{t+1}$  but are not present in the current propagation graph  $g_t$ . These nodes are referred to as *global candidates*:

$$C''_{t+1} = \{v \in V_{G_{t+1}} | v \notin V_{g_t}\}.$$

By introducing the second type of nodes, we incorporate a restart mechanism that allows unselected nodes to receive consideration

during the node selection process. This approach strikes a balance between localized exploration around the existing key nodes and a global search across the entire candidate graph. Besides, to control the balance between these two types of candidates, a trade-off parameter  $\epsilon \in [0, 1]$  is introduced. At each step  $t$ , we either set  $C_{t+1} = C'_{t+1}$  with a probability of  $\epsilon$ , to locally explore the boundary of the current key propagation graph  $g_t$ , or set  $C_{t+1} = C''_{t+1}$  with a probability of  $(1 - \epsilon)$ , to restart the exploration from one of the other nodes that have not been selected before, enabling a global search across of the entire graph.

Next, if the parents of candidates exist in the current propagation graph  $g_t$ , we append the feature of its parents to each candidate. Specifically, for candidate  $v \in C_{t+1}$  with feature  $X[v]$ , and its parent  $v_p \in V_{g_t}$ ,  $(v_p, v) \in E_{G_{t+1}}$ , we augment the feature of  $v$  as follows:

$$X'[v] = X[v] \parallel H[v_p].$$

In cases where the parents of candidates do not exist in  $g_t$ , we simply pad their features with zeros. Then, we derive the probabilities  $\mathbf{p}_t$  using a fully connected layer followed by a softmax function:

$$\mathbf{p}_t = \text{softmax}(\text{FC}(X'[C_{t+1}])),$$

where  $X'[C_{t+1}]$  is the features of candidate nodes in  $C_{t+1}$ . Finally, based on the probability distribution  $\mathbf{p}_t$ , action  $a_t$  selects a new node  $v_t$  from  $C_{t+1}$  to be added to  $g_t$  with a probability of  $\text{Pr}[a_t]$ :

$$\text{Pr}[a_t = (v_t, e(v_t))] = \mathbf{p}_t[v_t], \forall v_t \in C_{t+1}.$$

If the parent  $u$  of  $v_t$  exists in  $g_t$ , we set  $e(v_t) = (u, v_t)$ ; otherwise, we set  $e(v_t) = (r, v_t)$  to highlight the importance of the root node  $r$ . The state  $g_t$  is updated by adding the newly selected node and edge in action  $a_t$ :

$$g_{t+1} = (V_{g_t} \cup v_t, E_{g_t} \cup e(v_t), X_{g_t} \cup X[v_t]).$$

ENS considers two types of candidates and introduces a trade-off parameter  $\epsilon$  to balance these two sets, which is similar to the restart probability in the random walk [40]. We either locally select the next nodes from the out-neighbors of the currently selected nodes with  $\epsilon$  probability, or restart from another node in the remaining part of the graph with  $(1 - \epsilon)$  probability, enabling a global exploration. Note that when restarting from other nodes, it is possible to select a node  $v_{t+1}$  that is not directly connected to the current key graph. In such cases, we add an edge between the root node  $r$  and  $v_{t+1}$ . This allows ENS to explore additional key propagation patterns without being limited by the structure of the graph.

### 3.4 Model Integration

In this section, we introduce the rewards designed to guide the training of ENS and CRG modules. These rewards are designed to guide the policy to select actions that result in the maximum expected accuracy improvement during the key graph generation process. To achieve this, we train a BiGCN [6] classifier  $f(\cdot)$  to make prediction for the event  $s = \{r, G\}$ :

$$\hat{\mathbf{p}}_s = f(G) = \text{softmax}(\text{BiGCN}(G)), \\ \hat{y} = \text{argmax}_y \hat{\mathbf{p}}_s[y].$$

For simplicity, we denote the output probability distribution on graph  $G$  as  $f(G)$ . The improvement in the probability score for the ground truth class is used to measure the performance gain.

**Algorithm 1:** Training Pipeline of KPG

---

**Input** : Set of events  $\{s_0, s_1, \dots\}$ , pre-trained BiGCN classifier  $f(\cdot)$ , maximum step  $L$

**Output**: Key propagation graph for each event,  $\pi_S, \pi_R$

- 1 Initialize  $\pi_S, \pi_R$
- 2 **for each epoch do**
- 3     **for each batch do**
- 4         **for step  $t = 0$  to  $L$  do**
- 5              $G_{t+1} \leftarrow \pi_R(G_t)$
- 6              $\mathbf{p}_t \leftarrow \pi_S(G_{t+1}, g_t)$
- 7             Sample action  $a_t = (v_t, e(v_t))$  based on  $\mathbf{p}_t$
- 8             Transfer to state
- 9              $g_{t+1} = (V_{g_t} \cup v_t, E_{g_t} \cup e(v_t), \mathbf{X}_{g_t} \cup \mathbf{X}[v_t])$
- 10            Train  $\pi_S$  using Eq. 5 with  $\pi_R$  fixed
- 10            Train  $\pi_R$  using Eq. 2 with  $\pi_S$  fixed

---

**CRG Training.** Recap from 3.2, CRG is designed based on CVAE [35], aiming to generate coherent and reliable responses that align with the contextual information in the graph, fulfilling objectives (i) and (ii). Besides, CRG aims to generate informative responses that contribute to improving the model performance on rumor classification, which corresponds to objective (iii). To achieve this, we design the reward based on the improvement of classification obtained by replacing the input textual features with the reconstructed responses. Let  $y_s$  denote the ground-truth label of event  $s$ . The reward for CRG is defined as follows:

$$R_{\pi_R}^{(t)} = e^{-(f(g'_t)[y_s] - f(g_t)[y_s])}, \quad (1)$$

where  $g_t$  and  $g'_t$  are the key propagation graphs with original features and reconstructed features, respectively,  $f(g_t)[y_s]$  is the prediction score based on graph  $g_t$  for the class  $y_s$ . If the generated responses are informative and contribute to the improved classification confidence, we get  $R_{\pi_R}^{(t)} < 1$ , encouraging the module to maintain its well-trained state. Otherwise, we get  $R_{\pi_R}^{(t)} \geq 1$  to push the module away from the current unsatisfactory state. Besides, following [35], we apply the stochastic gradient variational Bayes framework to optimize the reconstruction error and the KL divergence between the variational distribution and the prior distribution. The loss function of CRG is defined as follows:

$$\mathcal{L}_{\pi_R}^{(t)} = R_{\pi_R}^{(t)} \cdot \Sigma(\mathbb{E}_{q_\phi(z|\mathbf{h}_u, \mathbf{h}_v)}[\log p_\theta(\mathbf{h}_v|z, \mathbf{h}_u)] - KL(q_\phi(z|\mathbf{h}_u, \mathbf{h}_v) \| p_\theta(z|\mathbf{h}_u))). \quad (2)$$

**ENS Training.** The reward for ENS aims to generate a more discriminative key propagation graph after adding the new node. To achieve this, we design the reward of ENS from two aspects: (i) the improvement of the prediction score and (ii) the enhancement of future performance estimation. Specifically, we aim to obtain a higher prediction score on class  $y_s$  derived by classifier  $f(\cdot)$  on the updated key graph  $g_{t+1}$  compared to  $g_t$ . Meanwhile, we aim to maximize the future performance of  $g_{t+1}$  in the subsequent steps. To simulate future actions, we utilize a modified Rollout [5] to select up to  $(l-1)$  additional nodes from the current candidate set. These  $l$  nodes, including the selected one, are incrementally added to the

current key graph  $g_t$ , simulating the potential future actions over the next  $l$  steps. We combine the current prediction score and the future prediction scores to calculate an overall score for the updated key graph  $g_{t+1}$ :

$$r_{t+1} = \frac{1}{2} \left( f(g_{t+1})[y_s] + \frac{1}{l} \left( \sum_{i=1}^l f(\hat{g}_{t+i})[y_s] \right) \right),$$

where  $\hat{g}_{t+i}$  is the estimated future graph after  $i$  steps. The reward for ENS is defined as the margin between two scores:

$$R_{\pi_S}^{(t)} = e^{-(r_{t+1} - r_t)}. \quad (3)$$

Similarly to the rewards in CRG, if the performance is improved after action  $a_t$ , we get  $R_{\pi_S}^{(t)} < 1$ . Additionally, we introduce another reward to penalize the module if the classification performance on the current key propagation graph is unsatisfactory:

$$\bar{R}_{\pi_S}^{(t)} = 1.5 - f(g_{t+1})[y_s]. \quad (4)$$

If the prediction score on class  $y_s$  is lower than 0.5, we have  $\bar{R}_{\pi_S}^{(t)} \geq 1$ , penalizing the entire module and urging it to output a higher prediction score for class  $y_s$ . The final loss of ENS is derived by combining the cross-entropy loss of the GCN model:

$$\mathcal{L}_{\pi_S}^{(t)} = \bar{R}_{\pi_S}^{(t)} \cdot R_{\pi_S}^{(t)} \cdot L_{CE}. \quad (5)$$

**Training Pipeline.** Both ENS and CRG modules are interdependent on each other within the KPG framework. On the one hand, ENS relies on CRG to generate new responses, ensuring that there are enough nodes in the candidate set to select from. On the other hand, CRG requires ENS to provide effective context-response pairs to capture the latent variable distribution of responses accurately. Therefore, we employ an alternative training approach that allows an end-to-end learning of both modules. Specifically, we first fix CRG  $\pi_R$  and update ENS  $\pi_S$ . This is achieved by minimizing  $\mathcal{L}_{\pi_S}$  using Eqn. 5 through policy gradient [39]. Next, we fix ENS  $\pi_S$  and update CRG  $\pi_R$  by minimizing  $\mathcal{L}_{\pi_R}$  using Eqn. 2. This iterative process is repeated until the early stop condition is met or the maximum number of steps is reached. Algorithm 1 summarizes the learning pipeline of KPG.

To enhance generalization ability and mitigate over-fitting, we adopt batch training and the early stop strategy. The final key propagation graphs are used to train a new BiGCN classifier for downstream rumor detection tasks. Following GACL [38], we concatenate the texts of the source post and comments in the propagation graph as the input text for a BERT classifier [9]. The results from two classifiers are fused using the mean operation to derive the final classification results. Besides, we feed the training events to the model in descending order based on the sizes of their propagation graphs. This strategy ensures that both ENS and CRG can learn from informative propagation patterns at the beginning stage and better handle limited-spread events with small graphs.

**Time Complexity.** The time complexity of KPG per epoch is  $O(L(Mh + Nh^2))$ , where  $N$  and  $M$  denote the total nodes and edges across all graphs, respectively,  $L$  is the maximum generation step number, and  $h$  is the dimension of hidden layers. The overall cost is primarily determined by the step number  $L$  and the cost of the GCN model. In addition, the step number  $L$  is a tunable parameter that can be adjusted to strike a balance between processing time

**Table 2: Statistic of datasets. NR means non-rumors; FR means false rumors; TR means true rumors; UR means unverified rumors;  $|V|$  is the number of posts in each event.**

Statistic	Twitter15	Twitter16	PHEME	Weibo22
# events	1,490	818	3,720	4,174
# NR	374	205	1,860	2,087
# FR	370	205	1,860	2,087
# TR	372	205	0	0
# UR	374	203	0	0
# posts	41,194	18,618	67,238	961,962
# users	34,668	16,805	34,287	705,831
Avg. $ V $	28	23	18	230
Med. $ V $	16	13	15	7
Max $ V $	304	250	346	30,791
Min $ V $	1	1	2	1

and model accuracy. Our empirical results on the Twitter16 dataset in Table 6 show that KPG achieves superior classification accuracy compared to other baseline methods, even with small  $L$  values.

## 4 EXPERIMENT

In this section, we compare our KPG against 11 state-of-the-art competitors on 4 datasets. We also conduct early stage rumor detection and the ablation study to demonstrate the effectiveness of each component of KPG. Finally, we perform the parameter analysis to examine the impact of the parameters on the model performance.

### 4.1 Datasets

We evaluate KPG on three real-world benchmark datasets: Twitter15 [29], Twitter16 [29], and PHEME [61]. Twitter15 and Twitter16 are collected from the Twitter platform and divided into four rumor classes: *non-rumor (NR)*, *true rumor (TR)*, *false rumor (FR)*, and *unverified rumor (UR)*. The PHEME dataset is also a Twitter dataset related to five events and annotated with two labels: *rumor (R)* and *non-rumor (NR)*. All three datasets are commonly used in existing research studies [6, 30, 38] on rumor detection.

The released Weibo dataset used in [6, 28] is missing critical information required for several baselines, including original comment text and author details. However, these details cannot be fully recovered as there are many deleted user accounts and posts on Weibo. In addition, the propagation patterns and topics of rumor in real-world social networks have evolved rapidly. Considering these aspects, we have constructed a new dataset **Weibo22**. Events in Weibo22 are collected from Sina Weibo, which is one of the biggest social media platforms in China. The time period covered by the events in Weibo22 ranges from November 2019 to March 2022, with more than half of the events related to the COVID-19 pandemic. Specifically, the events in Weibo22 are divided into two classes, rumor and non-rumor, with the information provided by Weibo Community Management Center [4] and China Internet Joint Rumor Debunking Platform [2]. By using the Weibo API [3], we collect 4,174 source posts with 960 thousand microblogs, including reposts and comments in their propagation graphs. For each microblog, we also collect the user profile of the author, including the number of followers, the number of friends, verification status,

verification type, verification reason, etc. Detailed statistics of these four datasets are shown in Table 2.

### 4.2 Experimental Settings

**Baselines.** We compare KPG with eleven state-of-the-art baselines.

- BERT [9]: a powerful pre-trained language model based on bidirectional transformers. Following [38], we concatenate the source post and all comment posts in the same event as the input texts to fine-tune a BERT-based classifier;
- RvNN [30]: it employs tree-structured RNNs with GRUs to extract representations from the propagation structure in bottom-up and top-down manners;
- BiGCN [6]: a GCN-based model that learns features from both propagation and dispersion structures;
- EBGCN [44]: it uses a Bayesian approach to adjust the weights of uncertain relations and enforces consistency on latent relations using an edge-wise training framework;
- RDEA [12]: a contrastive self-supervised learning based method with event augmentation;
- GACL [38]: it designs graph perturbation methods based on adversarial and supervised contrastive learning;
- TrustRD [24]: it incorporates self-supervised learning and a Bayesian network to derive trustworthy predictions;
- SMG [47]: it learns graph representations from a sequence of subgraphs to better capture task-relevant substructures and skip noisy parts;
- AdaSNN[21]: it generates critical subgraphs with a bi-level mutual information enhancement mechanism optimized in the reinforcement learning framework;
- GLAN [52]: it learns local semantic and global structural information via attention mechanisms on the heterogeneous graph;
- SMAN [53]: it adopts a structure-aware multi-head attention module on the heterogeneous graph to optimize the user credibility prediction and rumor detection task jointly;
- SBAG [13], it adopts a pre-trained MLP to capture social bot features in the propagation graph and uses it as a scorer to train a social bot-aware GNN for rumor detection.

Among the baseline models, BERT [9] is the only one that utilizes text features without propagation structures. GLAN, SMAN, and SBAG use additional user information in the constructed heterogeneous graphs. Other competitors, along with our KPG, do not use any user information, but only the propagation graphs in rumor detection. Following [6, 12, 38, 44], we adopt Accuracy (Acc.) and  $F_1$ -measure ( $F_1$ ) for each class as evaluation metrics, and we randomly split the datasets into five parts to conduct 5-fold cross-validation to obtain the final results. For each dataset, we use the same data split on all methods for fair comparison.

**Remark.** Note that the batch-wise averaging approach is used in several baselines [6, 12, 24, 38, 44]. However, this approach can lead to performance variance, particularly when the final batch is smaller than the others. For instance, consider a 110-record dataset with batch size 100, the accuracy is 0.8 for the first batch and 0.9 for the second batch. The batch-wise averaging yields a result of 0.85, obviously skewed to the smaller second batch. To ensure a stable and reliable evaluation, we exclude the batch-wise averaging for all baselines. Instead, we calculate the average accuracy across all

**Table 3: Results on four datasets. NR, FR, TR, UR and R represents for non-rumor, false rumor, true rumor, unverified rumor and rumor, respectively. Best and second-best results are highlighted with bold and underlined text. We exclude methods cannot finish detection with 7 days. The last column reports the average rank over all datasets and metrics of each method.**

	Twitter15					Twitter16					PHEME			Weibo22			Rank
	Acc.	NR- $F_1$	FR- $F_1$	TR- $F_1$	UR- $F_1$	Acc.	NR- $F_1$	FR- $F_1$	TR- $F_1$	UR- $F_1$	Acc.	R- $F_1$	NR- $F_1$	Acc.	R- $F_1$	NR- $F_1$	
BERT	0.784	0.841	0.771	0.811	0.714	0.753	0.804	0.660	0.837	0.699	0.816	0.809	0.815	0.887	0.888	0.886	11.3
RvNN	0.793	0.817	0.791	0.822	0.745	0.783	0.755	0.737	0.849	0.783	0.768	0.774	0.762	0.858	0.858	0.857	11.6
BiGCN	0.837	0.813	0.846	0.892	0.798	0.857	0.798	<b>0.836</b>	0.923	0.873	0.841	0.842	0.841	0.905	0.907	0.904	5.9
EBGCN	0.851	0.827	0.864	0.891	<u>0.825</u>	0.858	0.804	0.835	0.920	<u>0.874</u>	0.839	0.840	0.837	0.870	0.876	0.864	6.4
RDEA	0.860	0.872	0.866	0.888	0.815	0.868	0.861	0.817	0.920	0.871	0.838	0.840	0.837	<u>0.918</u>	<u>0.920</u>	<u>0.917</u>	5.1
GACL	0.785	0.877	0.740	0.780	0.738	0.758	0.814	0.686	0.801	0.719	0.836	0.839	0.833	0.885	0.884	0.886	10.2
TrustRD	<u>0.866</u>	0.875	<u>0.871</u>	<u>0.896</u>	0.821	0.869	0.844	0.827	<u>0.929</u>	0.874	<u>0.846</u>	0.846	<u>0.846</u>	<u>0.918</u>	<u>0.920</u>	<u>0.917</u>	3.1
SMG	0.828	0.861	0.840	0.869	0.736	0.841	0.812	0.812	0.898	0.839	0.830	0.830	0.830	-	-	-	9.1
AdaSNN	0.798	0.763	0.767	0.844	0.772	0.792	0.711	0.783	0.871	0.800	0.820	0.811	0.827	-	-	-	10.8
GLAN	0.827	0.820	0.839	0.871	0.779	0.831	0.756	0.805	0.923	0.843	0.845	<u>0.849</u>	0.840	0.902	0.903	0.902	7.4
SMAN	0.853	<u>0.894</u>	0.851	0.860	0.806	0.853	<u>0.867</u>	0.788	0.914	0.842	0.836	0.837	0.835	0.911	0.912	0.909	6.6
SBAG	0.862	0.876	0.862	0.887	0.821	<u>0.870</u>	<u>0.863</u>	<b>0.836</b>	0.913	0.866	0.841	0.842	0.841	0.912	0.912	0.911	4.4
KPG	<b>0.893</b>	<b>0.921</b>	<b>0.898</b>	<b>0.903</b>	<b>0.847</b>	<b>0.889</b>	<b>0.894</b>	<b>0.836</b>	<b>0.930</b>	<b>0.896</b>	<b>0.859</b>	<b>0.863</b>	<b>0.854</b>	<b>0.949</b>	<b>0.949</b>	<b>0.948</b>	1.0

**Table 4: Ablation study on Twitter16.**

	Acc.	NR- $F_1$	FR- $F_1$	TR- $F_1$	UR- $F_1$
KPG	<b>0.889</b>	<b>0.894</b>	<b>0.836</b>	<b>0.930</b>	<b>0.896</b>
KPG\ens	0.865	0.882	0.810	0.910	0.855
KPG\crg	0.861	0.878	0.806	0.908	0.849
KPG\reward	0.865	0.880	0.808	0.914	0.855

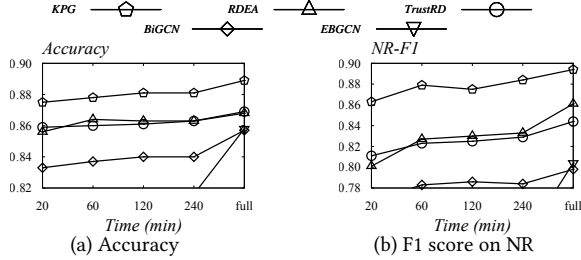


**Figure 2: Early stage rumor detection on Twitter16.**

data points in each epoch, mitigating any impact from variations in the final batch size.

**Parameter Setting.** We set the maximum step of the key propagation graph generation equal to  $\tau$  times the median size of the original graphs in each dataset, and we utilize grid search to set  $\tau$  from  $\{2^1, 2^2, 2^3\}$ . For Weibo22, considering that the median size of the original graphs is much smaller than the average size, we add an additional choice,  $s_{avg}$ , to the search list, where  $s_{avg}$  is the average size of the original graphs. We set the threshold of candidates  $\gamma = 5$  in CRG. We set the maximum step of rollout in ENS to 10, and the trade-off parameter between two candidate sets  $\epsilon = 0.8$ . Our KPG is optimized by Adam algorithm [18]. The learning rate is initialized to  $5 \times 10^{-4}$  and gradually decreases during training with a decay rate of  $10^{-4}$ . The dimension of hidden feature vectors in all modules is set to 64, and the batch size is set to 128.

### 4.3 Experimental Results

Table 3 shows the performance of all competitors on four real-world datasets. As we can observe, our KPG consistently achieves the best accuracy across all four datasets, which indicates the effectiveness

and generalization capability of our proposed RL-based key propagation graph generation method. On the Twitter15 and Twitter16 datasets, our KPG model outperforms the second-best results by achieving an increase of 2.7% and 2.7% in the  $F_1$  score for the non-rumor class, respectively. Furthermore, on the PHEME and Weibo22 datasets, KPG leads by 1.4% and 2.9% in the  $F_1$  score for the rumor class over the second-best performances.

Besides, our KPG model achieves the highest average ranking, illustrating its superior ability to generalize across diverse datasets and metrics. Specifically, compared to the model with the second highest average rank, TrustRD, KPG takes the lead by 2.7% and 2% on Twitter15 and Twitter16 datasets in terms of accuracy, respectively. Furthermore, KPG still outperforms models that use additional user information, including GLAN, SMAN, and SBAG. Compared with these three models, KPG takes the lead by up to 6.6% on Twitter15 and 5.8% on Twitter16 in terms of accuracy, which again shows the effectiveness of KPG.

On our newly crawled dataset, Weibo22, our KPG outperforms all other competitors in terms of all metrics. Compared with the second best baseline on Weibo22 dataset, KPG takes a lead by 3.1%, 2.9%, and 3.1% in terms of accuracy,  $F_1$  score on rumor, and  $F_1$  score on non-rumor, respectively, which again demonstrates that our key graph generation method can effectively reduce the noise while exploring more useful information.

### 4.4 Early Stage Rumor Detection

We also conduct experiments to validate the performance of KPG when detecting rumors in the early stage of spreading. We set a temporal threshold  $\Delta$  to filter nodes within each propagation graph in the dataset. Specifically, for every node in a propagation graph, we compute the time difference between the comment (or retweet) publication time of the node and the creation time of the root claim. Nodes with a time difference less than  $\Delta$  are kept, while those exceeding  $\Delta$  are excluded. We conduct the experiment with varying temporal thresholds  $\Delta \in \{20, 60, 120, 240\}$  minutes. Besides, we compare our KPG with the top four baselines in terms of average rank, excluding methods that require additional author information. The results of TrustRD, RDEA, BiGCN, EBGCN, and KPG in terms of accuracy and  $F_1$  score on non-rumor events are presented in

**Table 5: Results with varying  $\epsilon$  on Twitter16.**

$\epsilon$	1.0	0.8	0.6	0.4	0.2	0.0
Acc.	0.880	0.889	0.880	0.878	0.880	0.880
NR- $F_1$	0.884	0.894	0.881	0.884	0.880	0.888
FR- $F_1$	0.831	0.836	0.827	0.824	0.831	0.827
TR- $F_1$	0.922	0.930	0.927	0.922	0.924	0.923
UR- $F_1$	0.884	0.896	0.885	0.882	0.884	0.883

**Table 6: Results with varying  $\tau$  and  $l$  on Twitter16.**

	$\tau$				$l$		
	0	$2^1$	$2^2$	$2^3$	0	5	10
Acc.	0.832	0.875	0.883	0.889	0.879	0.872	0.889
NR- $F_1$	0.763	0.878	0.896	0.896	0.891	0.870	0.894
FR- $F_1$	0.819	0.825	0.824	0.836	0.822	0.823	0.836
TR- $F_1$	0.887	0.923	0.932	0.930	0.919	0.918	0.930
UR- $F_1$	0.859	0.872	0.880	0.896	0.882	0.875	0.896

Figure 2. The results of  $F_1$  scores on other three classes are similar to that of NR class and thus are omitted.

As we can see, at the early stage of spreading, the textual feature and topology information contained in the propagation graphs shrink and the performance of rumor detection generally decreases. However, the performance of our KPG consistently surpasses other baselines with varying  $\Delta$ . Specifically, the performance of KPG with  $\Delta = 20$  exceeds that of TrustRD, the second-best baseline, in both accuracy and  $F_1$  score for the non-rumor class, even when TrustRD utilizes full propagation graphs. The superior performance demonstrates again the effectiveness of our KPG, especially the CRG module, which generates realistic and informative responses and plays a key role in early stage rumor detection.

#### 4.5 Ablation Study and Parameter Analysis

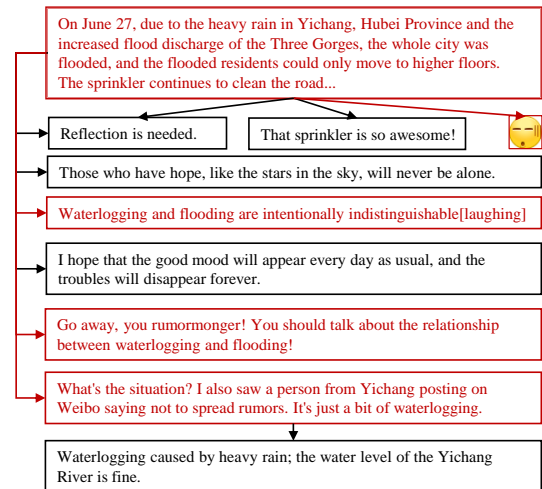
In this section, we first examine the effectiveness of each submodule, and then analyze the effects of hyperparameters in KPG.

**Ablation Study.** We conduct experiments to show the effectiveness of each key component of KPG. To achieve this, we implement the following three variants of KPG:

- KPG\ens: it reduces the ENS module to randomly selecting a node from the out-neighbors of the existing nodes;
- KPG\crg: it removes the CRG module and stops generating extra candidate nodes for small propagation graphs;
- KPG\reward: it eliminates rewards defined in Eqns. 1, 3, and 4.

Table 4 reports the results of KPG and three variant models on the Twitter16 dataset. The results on other datasets are similar to that on Twitter16 and thus are omitted. As we can observe, the absence of any component leads to a decrease in rumor detection performance. On the one hand, the decrease demonstrates the effectiveness of each module. On the other hand, the performance gap exhibits the importance of synergy of all three components.

**The Effect of Parameter  $\epsilon$  in Candidate Selection.**  $\epsilon \in [0, 1]$  is a trade-off parameter between local candidates and global candidates. Larger  $\epsilon$  indicates a larger probability for ENS to select the next node from the local neighbors of currently selected nodes, while smaller  $\epsilon$  indicates a larger probability to globally select from the

**Figure 3: An example of the generated propagation graph.**

nodes that have not been selected. We vary the parameter  $\epsilon$  from 0 to 1 and report the corresponding results on Twitter16 in Table 5. The results on other datasets are similar to that on Twitter16 and thus are omitted. In general, the model performance is influenced by the balance between local and global exploration. Specifically, on Twitter16, optimal performance is observed when  $\epsilon = 0.8$ . A similar performance distribution is noted across other datasets. Therefore, we set  $\epsilon = 0.8$  for KPG on all datasets in our experiments.

**The Effect of the Maximum Generation Steps.** Table 6 presents the rumor detection results on Twitter16 with varying  $\tau$ , which controls the max size of the generated key propagation graph. Specifically, we set the maximum generation steps as  $\tau$  times the median size of original graphs, where  $\tau$  is set from  $\{0, 2^1, 2^2, 2^3\}$ . When  $\tau = 0$ , only the root node is used for classification. As we can observe, the performance of KPG is the worst across all metrics, highlighting the significance of utilizing propagation graphs. As  $\tau$  increases, there is a general performance improvement across all metrics. When  $\tau = 2^3$ , KPG achieves the peak performance on Twitter16. This can be attributed to the relatively small average graph size in the Twitter16 dataset. The results of the ablation study also support this observation. Without the CRG component, reaching the maximum generation step becomes challenging, resulting in the most significant performance decline among three variants. Compared with other baselines, our KPG exhibits superior accuracy across various  $\tau$  values, even when  $\tau$  is relatively small, such as  $2^1$ .

**The Effect of the Maximum Step  $l$  in Modified Rollout.** Table 6 also reports the performance on Twitter16 with varying  $l$ , denoting the maximum steps of the Rollout when deriving the rewards for ENS. We conduct experiments with  $l \in \{0, 5, 10\}$ . As we can observe, the model performance peaks at  $l = 10$ , which demonstrates the effectiveness of evaluating each node from a long-term perspective via the modified Rollout.

#### 4.6 Case Study

To illustrate how our KPG works, we present the key propagation graph of a widespread rumor [1] from the Weibo22 dataset in Figure

3. With the original propagation graph, the event cannot be correctly classified by BiGCN. However, with the key graph generated by our KPG, it can be correctly identified as a rumor. Observations reveal that KPG selects nodes (highlighted in red) that enhance the discriminative capability of rumor detection, while disregarding irrelevant and noisy nodes. In particular, strong emotional responses are selected to refute the rumor.

## 5 CONCLUSION

In this paper, we propose KPG, a reinforcement learning-based model for rumor detection, comprised of two components: ENS and CRG. With the two modules cooperating together, the KPG identifies indicative substructures for events with noisy propagation information and generates realistic, reliable, and informative responses for events with insufficient propagation. The two components are trained alternately in an end-to-end framework under the guidance of our carefully designed rewards to improve the discriminative ability of generated key propagation graphs. Extensive experiments on four real-world datasets demonstrate that KPG achieves state-of-the-art performance. In addition, we construct a new dataset, Weibo22, containing posts with more recent dates and topics, which may contribute to the development of rumor detection-related research.

## REFERENCES

- [1] A rumor. [https://m.thepaper.cn/newsDetail\\_forward\\_8568258](https://m.thepaper.cn/newsDetail_forward_8568258).
- [2] China Internet Joint Rumor Debunking Platform. <https://www.piyaoo.org.cn/>.
- [3] Weibo API. <https://open.weibo.com/wiki/API>.
- [4] Weibo Community Management Center. <https://service.account.weibo.com/>.
- [5] D.P. Bertsekas. 1999. Rollout algorithms: an overview. In *Proceedings of the 38th IEEE Conference on Decision and Control*, Vol. 1. 448–449 vol.1.
- [6] Tian Bian, Xi Xiao, Tingyang Xu, Peilin Zhao, Wenbing Huang, Yu Rong, and Junzhou Huang. 2020. Rumor Detection on Social Media with Bi-Directional Graph Convolutional Networks. In *AAAI*. 549–556.
- [7] Kyunghyun Cho, Bart van Merriënboer, Dzmitry Bahdanau, and Yoshua Bengio. 2014. On the Properties of Neural Machine Translation: Encoder–Decoder Approaches. In *Proceedings of SSSST-8, Eighth Workshop on Syntax, Semantics and Structure in Statistical Translation*. Association for Computational Linguistics.
- [8] Jian Cui, Kwanwoo Kim, Seung Ho Na, and Seungwon Shin. 2022. Meta-Path-based Fake News Detection Leveraging Multi-level Social Context Information. In *CIKM*. 325–334.
- [9] Jacob Devlin, Ming-Wei Chang, Kenton Lee, and Kristina Toutanova. 2019. BERT: Pre-training of Deep Bidirectional Transformers for Language Understanding. In *NAACL-HLT*. 4171–4186.
- [10] Yajuan Duan, Zhimin Chen, Furu Wei, Ming Zhou, and Heung-Yeung Shum. 2012. Twitter Topic Summarization by Ranking Tweets using Social Influence and Content Quality. In *COLING*. 763–780.
- [11] Xiaojie Guo and Liang Zhao. 2023. A Systematic Survey on Deep Generative Models for Graph Generation. *TPAMI* 45, 5 (2023), 5370–5390.
- [12] Zhenyu He, Ce Li, Fan Zhou, and Yi Yang. 2021. Rumor Detection on Social Media with Event Augmentations. In *SIGIR*. 2020–2024.
- [13] Zhen Huang, Zhilong Lv, Xiaoyun Han, Binyang Li, Menglong Lu, and Dongsheng Li. 2022. Social Bot-Aware Graph Neural Network for Early Rumor Detection. In *COLING*. 6680–6690.
- [14] Yiqiao Jin, Xiting Wang, Ruichao Yang, Yizhou Sun, Wei Wang, Hao Liao, and Xing Xie. 2022. Towards Fine-Grained Reasoning for Fake News Detection. In *AAAI*. AAAI Press, 5746–5754.
- [15] Mostafa Karimi, Arman Hasanzadeh, and Yang Shen. 2020. Network-principled deep generative models for designing drug combinations as graph sets. *Bioinformatics* 36 (2020), i445–i454.
- [16] Yash Khemchandani, Stephen O’Hagan, Soumitra Samanta, Neil Swainston, Timothy J. Roberts, Danushka Bollegala, and Douglas B. Kell. 2020. DeepGraphMolGen, a multi-objective, computational strategy for generating molecules with desirable properties: a graph convolution and reinforcement learning approach. *J. Cheminformatics* 12, 1 (2020), 53.
- [17] Ling Min Serena Khoo, Hai Leong Chieu, Zhong Qian, and Jing Jiang. 2020. Interpretable Rumor Detection in Microblogs by Attending to User Interactions. In *AAAI*. 8783–8790.
- [18] Diederik P. Kingma and Jimmy Ba. 2015. Adam: A Method for Stochastic Optimization. In *ICLR*.
- [19] Diederik P. Kingma and Max Welling. 2014. Auto-Encoding Variational Bayes. In *ICLR*.
- [20] Thomas N Kipf and Max Welling. 2016. Semi-supervised classification with graph convolutional networks. In *ICLR*.
- [21] Jianxin Li, Qingyun Sun, Hao Peng, Beining Yang, Jia Wu, and Philip S. Yu. 2023. Adaptive Subgraph Neural Network With Reinforced Critical Structure Mining. *IEEE Trans. Pattern Anal. Mach. Intell.* 45, 7 (2023), 8063–8080.
- [22] Quanzhi Li, Qiong Zhang, and Luo Si. 2019. Rumor Detection by Exploiting User Credibility Information, Attention and Multi-task Learning. In *ACL*. 1173–1179.
- [23] Yujia Li, Oriol Vinyals, Chris Dyer, Razvan Pascanu, and Peter W. Battaglia. 2018. Learning Deep Generative Models of Graphs. *CoRR* abs/1803.03324 (2018).
- [24] Leyuan Liu, Junyi Chen, Zhangtao Cheng, Wenxin Tai, and Fan Zhou. 2023. Towards Trustworthy Rumor Detection with Interpretable Graph Structural Learning. In *CIKM 2023*. 4089–4093.
- [25] Zemin Liu, Qiheng Mao, Chenghao Liu, Yuan Fang, and Jianling Sun. [n.d.]. On Size-Oriented Long-Tailed Graph Classification of Graph Neural Networks. In *WWW 2022*. ACM, 1506–1516.
- [26] Yi-Ju Lu and Cheng-Te Li. 2020. GCAN: Graph-aware Co-Attention Networks for Explainable Fake News Detection on Social Media. In *ACL*. 505–514.
- [27] Guanghui Ma, Chunming Hu, Ling Ge, Junfan Chen, Hong Zhang, and Richong Zhang. 2022. Towards Robust False Information Detection on Social Networks with Contrastive Learning. In *CIKM*. 1441–1450.
- [28] Jing Ma, Wei Gao, Prasenjit Mitra, Sejeong Kwon, Bernard J. Jansen, Kam-Fai Wong, and Meeyoung Cha. 2016. Detecting Rumors from Microblogs with Recurrent Neural Networks. In *IJCAI 2016*. IJCAI/AAAI Press, 3818–3824.
- [29] Jing Ma, Wei Gao, and Kam-Fai Wong. 2017. Detect Rumors in Microblog Posts Using Propagation Structure via Kernel Learning. In *ACL*. 708–717.
- [30] Jing Ma, Wei Gao, and Kam-Fai Wong. 2018. Rumor Detection on Twitter with Tree-structured Recursive Neural Networks. In *ACL*. 1980–1989.
- [31] Mariya Popova, Mykhailo Shvets, Junier Oliva, and Olexandr Isayev. 2019. MolecularRNN: Generating realistic molecular graphs with optimized properties. *arXiv preprint arXiv:1905.13372* (2019).
- [32] Nir Rosenfeld, Aron Szanto, and David C. Parkes. 2020. A Kernel of Truth: Determining Rumor Veracity on Twitter by Diffusion Pattern Alone. In *WWW*. 1018–1028.
- [33] Victoria L. Rubin. 2010. On deception and deception detection: Content analysis of computer-mediated stated beliefs. In *ASIST*, Vol. 47. 1–10.
- [34] Fangzhou Shi, Shan You, and Chang Xu. 2019. Reinforced Molecule Generation with Heterogeneous States. In *ICDM*. 548–557.
- [35] Kihyuk Sohn, Honglak Lee, and Xinchen Yan. 2015. Learning Structured Output Representation using Deep Conditional Generative Models. In *NeurIPS*, Vol. 28.
- [36] Yun-Zhu Song, Yi-Syuan Chen, Yi-Ting Chang, Shao-Yu Weng, and Hong-Han Shuai. 2021. Adversary-Aware Rumor Detection. In *ACL/IJCNLP*, Chengqing Zong, Fei Xia, Wenjie Li, and Roberto Navigli (Eds.), Vol. *ACL/IJCNLP 2021*. 1371–1382.
- [37] Yongduo Sui, Xiang Wang, Jiancan Wu, Min Lin, Xiangnan He, and Tat-Seng Chua. 2022. Causal Attention for Interpretable and Generalizable Graph Classification. In *KDD*. ACM, 1696–1705.
- [38] Tienying Sun, Zhong Qian, Sujun Dong, Peifeng Li, and Qiaoming Zhu. 2022. Rumor Detection on Social Media with Graph Adversarial Contrastive Learning. In *WWW*. 2789–2797.
- [39] Richard S. Sutton, David A. McAllester, Satinder Singh, and Yishay Mansour. 1999. Policy Gradient Methods for Reinforcement Learning with Function Approximation. In *NeurIPS*. 1057–1063.
- [40] Hanghang Tong, Christos Faloutsos, and Jia-yu Pan. 2006. Fast Random Walk with Restart and Its Applications. In *Sixth International Conference on Data Mining (ICDM’06)*.
- [41] Rakshit Trivedi, Jiachen Yang, and Hongyuan Zha. 2020. GraphOpt: Learning Optimization Models of Graph Formation. In *ICML*, Vol. 119. 9603–9613.
- [42] Yaqing Wang, Fenglong Ma, Zhiwei Jin, Ye Yuan, Guangxu Xun, Kishlay Jha, Lu Su, and Jing Gao. 2018. EANN: Event Adversarial Neural Networks for Multi-Modal Fake News Detection. In *KDD*. 849–857.
- [43] Lingwei Wei, Dou hu, Wei Zhou, Xin Wang, and Songlin hu. 2022. Modeling the uncertainty of information propagation for rumor detection: A neuro-fuzzy approach. *IEEE Transactions on Neural Networks and Learning Systems* (2022).
- [44] Lingwei Wei, Dou Hu, Wei Zhou, Zhaoyuan Yue, and Songlin Hu. 2021. Towards Propagation Uncertainty: Edge-enhanced Bayesian Graph Convolutional Networks for Rumor Detection. In *ACL/IJCNLP (1)*. 3845–3854.
- [45] Penghui Wei, Nan Xu, and Wenji Mao. 2019. Modeling Conversation Structure and Temporal Dynamics for Jointly Predicting Rumor Stance and Veracity. In *EMNLP-IJCNLP*. 4786–4797.
- [46] Ke Wu, Song Yang, and Kenny Q. Zhu. 2015. False rumors detection on Sina Weibo by propagation structures. In *ICDE*, Johannes Gehrke, Wolfgang Lehner, Kyuseok Shim, Sang Kyun Cha, and Guy M. Lohman (Eds.). 651–662.
- [47] Mingqi Yang, Yanming Shen, Heng Qi, and Baocai Yin. 2021. Soft-mask: Adaptive Substructure Extractions for Graph Neural Networks. In *The Web Conference*

2021. 2058–2068.
- [48] Ruichao Yang, Xiting Wang, Yiqiao Jin, Chaozhuo Li, Jianxun Lian, and Xing Xie. 2022. Reinforcement Subgraph Reasoning for Fake News Detection. In *KDD*. 2253–2262.
- [49] Shuo Yang, Kai Shu, Suhang Wang, Renjie Gu, Fan Wu, and Huan Liu. 2019. Unsupervised Fake News Detection on Social Media: A Generative Approach. In *AAAI*. 5644–5651.
- [50] Jiaxuan You, Bowen Liu, Zhitao Ying, Vijay S. Pande, and Jure Leskovec. 2018. Graph Convolutional Policy Network for Goal-Directed Molecular Graph Generation. In *NeurIPS*. 6412–6422.
- [51] Jiaxuan You, Rex Ying, Xiang Ren, William L. Hamilton, and Jure Leskovec. 2018. GraphRNN: Generating Realistic Graphs with Deep Auto-regressive Models. In *ICML*, Vol. 80. 5694–5703.
- [52] Chunyuan Yuan, Qianwen Ma, Wei Zhou, Jizhong Han, and Songlin Hu. 2019. Jointly Embedding the Local and Global Relations of Heterogeneous Graph for Rumor Detection. In *ICDM*. 796–805.
- [53] Chunyuan Yuan, Qianwen Ma, Wei Zhou, Jizhong Han, and Songlin Hu. 2020. Early Detection of Fake News by Utilizing the Credibility of News, Publishers, and Users based on Weakly Supervised Learning. In *COLING*. 5444–5454.
- [54] Guixian Zhang, Rongjiao Liang, Zhongyi Yu, and Shichao Zhang. 2022. Rumour Detection on Social Media with Long-Tail Strategy. In *IJCNN*. 1–8.
- [55] Kaiwei Zhang, Junchi Yu, Haichao Shi, Jian Liang, and Xiaoyu Zhang. 2023. Rumor Detection with Diverse Counterfactual Evidence. In *Proceedings of the 29th ACM SIGKDD Conference on Knowledge Discovery and Data Mining, KDD 2023*. ACM, 3321–3331.
- [56] Qiang Zhang, Aldo Lipani, Shangsong Liang, and Emine Yilmaz. 2019. Reply-Aided Detection of Misinformation via Bayesian Deep Learning. In *WWW*. 2333–2343.
- [57] Tianxiang Zhao, Dongsheng Luo, Xiang Zhang, and Suhang Wang. 2022. TopoImb: Toward Topology-Level Imbalance in Learning From Graphs. In *Learning on Graphs Conference, LoG 2022 (Proceedings of Machine Learning Research, Vol. 198)*. PMLR, 37.
- [58] Xinyi Zhou, Apurva Mulay, Emilio Ferrara, and Reza Zafarani. 2020. ReCOVeRY: A Multimodal Repository for COVID-19 News Credibility Research. In *CIKM*. 3205–3212.
- [59] Xinyi Zhou and Reza Zafarani. 2019. Network-based Fake News Detection: A Pattern-driven Approach. *SIGKDD Explor.* 21, 2 (2019), 48–60.
- [60] Xinyi Zhou and Reza Zafarani. 2021. A Survey of Fake News: Fundamental Theories, Detection Methods, and Opportunities. *ACM Comput. Surv.* 53, 5 (2021), 109:1–109:40.
- [61] Arkaitz Zubiaga, Maria Liakata, and Rob Procter. 2016. Learning Reporting Dynamics during Breaking News for Rumour Detection in Social Media. *CoRR* abs/1610.07363 (2016).